Molecular Biology of the Cell
Vol. 15, 4877–4891, November 2004

Protein KinaseCδ-Calmodulin Crosstalk Regulates Epidermal Growth Factor Receptor Exit from Early Endosomes

Anna Lladó,*† Francesc Tebar,*† Maria Calvo,* Jemina Moretó,* Alexander Sorkin,‡ and Carlos Enrich*§

*Departament de Biologia Cellular, Facultat de Medicina, Universitat de Barcelona, 08036 Barcelona, Spain; and ‡Department of Pharmacology, Health Science Center, University of Colorado, Denver, CO 80262

Submitted February 13, 2004; Revised August 20, 2004; Accepted August 23, 2004
Monitoring Editor: Keith Mostov

We have recently shown that calmodulin antagonist W13 interferes with the trafficking of the epidermal growth factor receptor (EGFR) and regulates the mitogen-activated protein kinase (MAPK) signaling pathway. In the present study, we demonstrate that in cells in which calmodulin is inhibited, protein kinase C (PKC) inhibitors rapidly restore EGFR and transferrin trafficking through the recycling compartment, although onward transport to the degradative pathway remains arrested. Analysis of PKC isoforms reveals that inhibition of PKCδ with rottlerin or its down-modulation by using small interfering RNA is specifically responsible for the release of the W13 blockage of EGFR trafficking from early endosomes. The use of the inhibitor Gö 6976, specific for conventional PKCs (α, β, and γ), or expression of dominant-negative forms of PKCλ, ζ, or ε did not restore the effects of W13. Furthermore, in cells treated with W13 and rottlerin, we observed a recovery of brefeldin A tubulation, as well as transport of dextran-fluorescein isothiocyanate toward the late endocytic compartment. These results demonstrate a specific interplay between calmodulin and PKCδ in the regulation of the morphology of and trafficking from the early endocytic compartment.

INTRODUCTION

The early endosome is a highly complex and dynamic intracellular compartment involved in the sorting of endocytosed receptors and ligands, for receptor recycling or targeting to lysosomes; in addition, it participates in endosome–endosome fusion and fission events (Gruenberg, 2001). The identification of microdomains in early endosomes, together with specific molecular activities (i.e., phosphorylation of signaling proteins or ubiquitylation of receptors), suggests that sorting and exit (budding) from this compartment are finely regulated and further indicates that our knowledge of its molecular machinery is incomplete. Thus, in addition of proteins that might be involved in the formation of specific domains (domain organizers) such as Rab5, Rab4, or annexin 2, other components are also likely to be important for the integrated function of endosomal sorting and trafficking.

In a previous study, we demonstrated the importance of calmodulin in the regulation of early endocytic compartment morphology as well as in the trafficking and signaling of the epidermal growth factor receptor (EGFR) in this structure (Tebar *et al*., 2002). Now, we analyze the molecular mechanisms and the function of calmodulin in EGFR exit from early endosomes.

Calmodulin specifically interacts with the EGFR in a calcium-dependent manner (Martin-Nieto and Villalobo, 1998; Li *et al*., 2004). Mutations in the juxtamembrane domain (calmodulin-binding site) of the EGFR, or deletion of the basic segment (645–660 amino acids), inhibit this interaction; interestingly, this region contains the threonine 654, the target of protein kinase C (PKC). Calmodulin binding inhibits EGFR tyrosine kinase activity in vitro (San José *et al*., 1992) and PKC-induced phosphorylation at Thr654 (Lund *et al*., 1990; Bao *et al*., 2000); conversely, EGFR phosphorylation by PKC inhibits calmodulin binding.

Interfering with PKC phosphorylation seems to be a rather general mechanism for calmodulin action (as occurs with other PKC substrates: MARCKS, MacMARCKS, AKAP79, adducins, or GAP 43) (Jaken and Parker, 2000), which has at least two important consequences: first, a decrease in the free calmodulin concentration locally and second, the regulation of intracellular signaling.

However, PKC takes account of ubiquitous large family of serine/threonine protein kinases (PKC isoforms) whose activity is dependent upon lipid cofactors and regulators and that have been broadly involved in many cellular regulatory processes, including cytoskeleton rearrangements (Keenan and Kelleher, 1998), membrane trafficking, ion transport, signaling, and cell adhesion (Newton, 1997). In fact, as shown with calmodulin antagonists W7 and W13, it has been reported that activation of PKC with 12-*O*-tetradecanoylphorbol-13-acetate (TPA) leads to production of enlarged endosomes in the cell via a mechanism involving Rab5 and the homotypic fusion of endosomes (Aballay *et al*., 1999). Compared with W13, TPA does not affect the sorting rate of molecules from endosomes (Klausner *et al*., 1984). Apparently, the PKC-induced phosphorylation of the EGFR at threonine 654 is sufficient to direct incoming receptors to the recycling endosomes, whereas phosphorylation at ty-

Article published online ahead of print. Mol. Biol. Cell 10.1091/mbc.E04–02–0127. Article and publication date are available at www.molbiolcell.org/cgi/doi/10.1091/mbc.E04–02–0127.

† These authors contributed equally to this work.

§ Corresponding author. E-mail address: enrich@ub.edu.

rosine residues directs the receptor to the multivesicular bodies (MVB)/late endosomal compartment, in agreement with the close relationship between endocytosis, trafficking, sorting, and signaling events (Bao *et al*., 2000).

Various PKC isoforms have been implicated in the control of vesicle trafficking in the GLUT4 and Fcε R systems (Anderson and Olefsky, 1991; Liu *et al*., 2001) and also more recently PKCα and δ were shown to be required for Fcα R (CD89) trafficking to MHC class II compartments and Fcα R-mediated antigen presentation (Chen *et al*., 2004). Furthermore, different isoforms of PKC have been located in intracellular structures related to intracellular trafficking such as in caveolae, along the structures of the endocytic compartment, the Golgi complex and in lysosomes. The role of PKC in endocytosis, sorting, and/or trafficking is not completely understood but its activity seems important (Sanchez *et al*., 1998; Bao *et al*., 2000; Prevostel *et al*., 2000; Larocca *et al*., 2002; Ridge *et al*., 2002; Becker and Hanunn, 2003). In the present study, the activated form of PKCδ has been located in endosomal fractions isolated from COS cells, and by using inhibitors and/or the small interfering RNA (siRNA)-mediated down-regulation we demonstrate that in the absence of calmodulin, PKCδ is specifically involved in the regulation of EGFR exit from the early endocytic compartment.

MATERIALS AND METHODS

Reagents

Mouse receptor-grade epidermal growth factor (EGF), peroxidase type VI from horseradish (HRP), brefeldin A (BFA), and W13 were purchased from Sigma Chemical (Madrid, Spain). TPA, bisindolylmaleimide I (BIM), Gö 6976, and rottlerin were from Calbiochem (Merck Eurolab, Darmstadt, Germany). EGF, dextran, and transferrin conjugated with tetramethylrhodamine B isothiocyanate (TRITC) or fluorescein isothiocyanate (FITC) were from Molecular Probes (Eugene, OR). A monoclonal antibody against the extracellular domain of the EGFR was obtained from American Type Culture Collection (Rockville, MD); anti-PKCδ and early endosomal antigen 1 (EEA1) monoclonal antibodies were from BD Transduction Laboratories (Lexington, KY); anti-actin monoclonal antibodies were from ICN Iberica, Barcelona, Spain; the rabbit polyclonal PKCδ and anti-Rab5 antibodies were from Santa Cruz Biotechnology (Santa Cruz, CA); and the rabbit polyclonal phospho-PKCδ (Ser643) antibody was from Cell Signaling Technology (New England Biolabs, Hitchin, United Kingdom). The mouse monoclonal anti-lysobisphosphatidic acid (LBPA) was kindly donated by Dr. Jean Gruenberg (University of Geneva). Peroxidase-labeled antibodies and SDS-PAGE molecular weight markers were from Bio-Rad (Hercules, CA). ^{125}I-EGF was prepared as described in Carter and Sorkin (1998) or purchased from Amersham Biosciences UK (Little Chalfont, Buckinghamshire, England).

Cell Culture

Green monkey kidney cells (COS-1) were grown in DMEM containing 10% fetal calf serum (FCS), pyruvic acid, antibiotics, and glutamine. DMEM and FCS were purchased from Biological Industries (Beit Haemek, Israel). Cells were grown to ~90% confluence for cellular fractionation or radioactivity experiments, or 50% confluence for immunofluorescence experiments. In some experiments, we also used porcine aortic endothelial (PAE) (EGFR-green fluorescent protein [GFP]) cells or HeLa cells (when siRNAs were used).

Transfection of EGFR-GFP, GFP-Dominant-Negative PKC Isoforms, and siRNAs

Expression vector encoding kinase-inactivated GFP-PKCδ (K378R) was a gift of Dr. C. Larsson (Lund University, Lund, Sweden) (Ling *et al*., 2004). The generation of plasmids containing dominant-negative PKCλ, ζ, and ε (kindly provided by Dr. Jorge Moscat, Centro deBiología Molecular, Severo Ochoa, Madrid, Spain) has been described previously (Diaz-Meco *et al*., 1993; Diaz-Meco *et al*., 1996; Uberall, 1996). To obtain a GFP-dominant-negative atypical PKC (aPKC), an *Eco*RI/*Apa*I fragment was excised from pcDNA3-dominant negative aPKC and ligated to *Eco*RI/*Apa*I digested pEGFP-N2. Similarly, to generate GFP-dominant-negative PKCε, an *Eco*RI fragment was excised from pcDNA3-dominant negative novel PKC (nPKC)ε and ligated to *Eco*RI digested pEGFP-N2. Transient expression was performed using Polyfect or Effectene (QIAGEN, Valencia, CA) and the cells were used for experiments 24–48 h after transfection.

A cell line of PAE cells stably expressing GFP-EGFR wt was established using standard single-cell cloning and G418 selection procedures (Carter and Sorkin, 1998). PAE cell lines were grown in F-12 medium containing 10% fetal bovine serum, antibiotics, pyruvic acid, and glutamine.

siRNAs duplexes were synthetized and purified by QIAGEN as described by Yoshida *et al*. (2003). The siRNA sequences for targeting PKCδ were PKCδ siRNA1 (5′-GAUGAAGGAGGCGCUCAGTT-3′) and PKCδ siRNA2 (5′-GGCUGAGUUCUGGCUGGACTT-3′). We found that optimal conditions were achieved using 10 μl of 20 μM solution of the PKCδ siRNA2 and transfecting HeLa cells in six-well plates (40–50% confluence; 2 ml of DMEM + 10% FCS/well) with 5 μl of Lipofectamine 2000 reagent (Invitrogen, Carlsbad, CA) in 250 μl of Opti-MEM medium for 6 h, following protocols provided by the manufacturer. Experiments were conducted 72 h after transfection. GFPsiRNA was used as a negative control (Hirai and Wang, 2002).

Immunofluorescence Staining

Cells grown on coverslips were incubated in binding medium (DMEM + 0.1% bovine serum albumin [BSA]) with different treatments, fixed with freshly prepared 4% paraformaldehyde for 12 min at room temperature and mildly permeabilized with phosphate-buffered saline (PBS) containing 0.1% Triton X-100, 0.1% BSA at room temperature for 3 min. Coverslips were then incubated in the same buffer, in which Triton X-100 was omitted, at room temperature for 1 h with the primary antibody, washed extensively, and then incubated with appropriate secondary antibodies labeled with FITC (Jackson Immunoresearch Laboratories, West Grove, PA) or Alexa Fluor 488 or 546 (Molecular Probes). Both primary and secondary antibody solutions were precleared by centrifugation at 14,000 × *g* for 10 min. After staining, the coverslips were mounted in Mowiol (Calbiochem). Images were collected using an inverted epifluorescence Axiovert 200M microscope (Carl Zeiss, Göttingen, Germany) equipped with a Photometric Cool Snap HQ camera, all controlled by Slide-Book 3.0.10.5 software (Intelligent Imaging Innovation, Denver, CO). Final analysis of deconvoluted images was performed using Adobe Photoshop software.

To ascertain the degree of colocalization of dextran-FITC (10,000 mol wt) and the late endosomal marker LBPA, after the treatment with W13 and rottlerin, double labeling was performed in cells fixed for 2 h at room temperature with 4% paraformaldehyde in 40 mM sodium phosphate/75 mM lysine buffer, pH 7.4, containing 9.1 mM sodium periodate and permeabilized with 0.1% saponin in 0.5% BSA/PBS-20 mM glycine for 10 min. Cells were processed for indirect immunofluorescence microscopy as described above. This procedure improves the retention of the fluid phase marker with the immunocytochemical detection (Pons *et al*., 2000).

Time-Lapse Fluorescence Confocal Microscopy

Time-lapse fluorescence confocal microscopy experiments were carried out using a Leica TCS SL laser-scanning confocal spectral microscope (Leica Microsystems Heidelberg, Manheim, Germany) with argon and HeNe lasers attached to a Leica DMIRE2 inverted microscope equipped with an incubation system with temperature and CO_2 control. For visualization of EGFR-GFP in EGF + W13 + BIM experiments, confocal images were acquired using a 63× oil immersion objective lens (numerical aperture 1.32), 488-nm laser line, excitation beam splitter RSP 500, and an emission range detection 500–610 nm. Images were acquired at 30-s intervals for 1–2 h, and optical sectioning was necessary to capture the whole signal. The excitation intensity was attenuated to 5% of the half-laser power to avoid significant photobleaching. Image treatment and movie assembly were performed using the Image Processing Leica Confocal Software.

Recycling and Degradation of ^{125}I-EGF

^{125}I-EGF recycling and degradation was measured as described previously (Kornilova *et al*., 1996). Briefly, cells in 35-mm culture dishes were incubated with 5 ng/ml ^{125}I-EGF for 7 min at 37°C and washed in cold DMEM. Noninternalized ^{125}I-EGF was removed from the cell surface by a 2.5-min acid wash (0.2 M sodium acetate, 0.5 M NaCl, pH 4.5). At this point cells are referred to as "^{125}I-EGF–loaded cells." Trafficking of ^{125}I-EGF-receptor complexes in these loaded cells was then initiated by incubating the cells in fresh binding medium containing 100 ng/ml unlabeled EGF and other reagents DMSO, W13 (10 μg/ml), BIM (5 μM), Gö 6976 (1 μM), and rottlerin (5 μM) at 37°C for 0–60 min. Excess of unlabeled EGF in the medium and at the cell surface prevented rebinding and reinternalization of recycled ^{125}I-EGF. At the end of the chase incubation, the medium was collected to measure the amount of intact and degraded ^{125}I-EGF by precipitation with trichloroacetic acid (TCA), and cells were incubated for 5 min with 0.2 M acetic acid (pH 2.8) containing 0.5 M NaCl at 4°C to determine the amount of surface-bound ^{125}I-EGF. Finally, cells were solubilized in 1 N NaOH to measure the amount of intracellular ^{125}I-EGF. The amount of recycled ^{125}I-EGF was estimated by summing the radioactivity counted on the cell surface and the TCA-precipitated radioactivity in the medium during chase incubation; the recycling rate was expressed as the ratio of this sum to the total EGF molecules. The degradation rate was calculated as the ratio of the amount of degraded ^{125}I-EGF (TCA soluble) in the medium to the amount of total radioactivity at each time point.

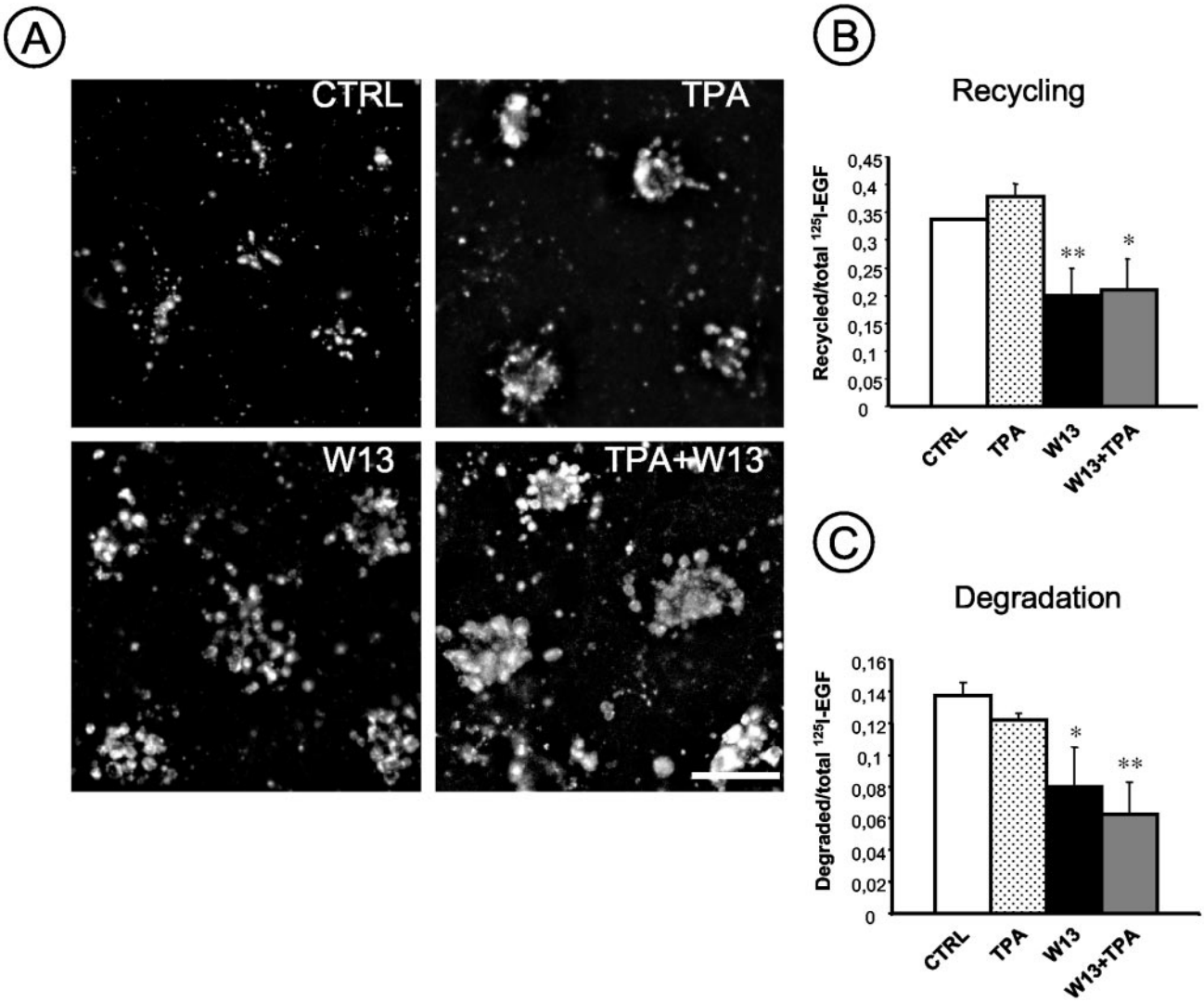

Figure 1. Calmodulin antagonist W13 and PKC activator TPA exert a synergistic effect on enlarged EGFR-positive endosome formation. Starved COS-1 cells were preincubated with W13 (10 μg/ml) and/or TPA (100 nM) for 30 min before EGF treatment (100 ng/ml) for 30 min at 37°C. (A) Cells grown on coverslips were fixed and stained with anti-EGFR (Ab225) followed by a goat anti-mouse secondary antibody labeled with FITC. Bar, 10 μm. After 7 min of ^{125}I-EGF (5 ng/ml) internalization, COS-1 cells were incubated in the presence of W13 (10 μg/ml) and/or TPA (100 nM) for 30 and 60 min to measure recycling (B) and degradation (C), respectively. Data in the histograms shows a mean of two independent experiments. Statistical significances of differences between controls and corresponding W13 treatments were determined using the Student's *t* test. *$P < 0.05$, **$P < 0.01$.

Ultrastructural Analysis

Two different approaches were undertaken to study the ultrastructure of endosomes in COS-1 cells in control and after the different treatments. First, cell monolayers on P100 dishes were rinsed with PBS and fixed with 2% paraformaldehyde and 2.5% glutaraldehyde in 0.1 M phosphate buffer for 1 h at room temperature. Cells were gently scraped, collected into the same buffer, and pelleted by centrifugation (5 min, 500 × *g*). After three rinses in 0.1 M phosphate buffer, pellets were postfixed in 1% OsO_4-0.8% FeCNK for 1 h 30 min. Finally, samples were embedded in Spurr (Sigma Chemical). Images taken from these samples were used for the stereological analysis. Similar to in our previous study (Apodaca *et al.*, 1994), structures of interest were considered those low-dense vacuolar structures clearly distinguishable from the rest of intracellular organelles (mitochondria, Golgi, and lysosomes).

Second, we also loaded the cells with HRP for 7 min to ascertain that enlarged aberrant structures (in COS cells treated with W13 or W13 + TPA) were early endosomes. After internalization of HRP, the cells were washed and immediately fixed by adding ice-cold 0.5% (vol/vol) glutaraldehyde in 200 mM cacodylate, pH 7.4, 1 mM $CaCl_2$, 0.5 mM $MgCl_2$, for 30 min at room temperature. Cells were rinsed with cacodylate buffer and then incubated for ~30 min with diaminobenzidine acid, dissolved in cacodylate buffer containing H_2O_2, at room temperature in the dark. Then, samples were rinsed, osmicated with 1% OsO_4, and embedded as described above (Apodaca *et al.*, 1994). Ultrathin sections were analyzed with a Jeol1010 electron microscope.

Procedures for Stereological Analysis of Endocytic Structures in COS Cells. Because the cells were pelleted and embedded in Spurr, which was randomly cut and mounted, the sections are considered to be isotropic, uniformly random sections. Grids were systematically screened, and ~80 regions with structures of interest (endosomes) were imaged, irrespective of their intracellular location. All structures were photographed at a primary magnification of 10,000×. For the measure of the area, we used the Quantity-One software (Bio-Rad) that calculates the area of profiles by following the perimeter of each endosome.

Calculation of the Mean Volume. The volume of individual objects may be calculated from transection data by the method described by Lindberg and Vorwerk (1970). The computing formula is:

$$\bar{v} = \beta \bar{A}^{3/2}$$

where $\bar{v}$ is the mean volume and $\bar{A}$ is the mean transection area. The values of β (choice of shape factor) for ellipsoids of various axial ratios *b/a* (*b*,

correspond to the width [minor axis] and *a*, the height [major axis] in micrometers) have been published in Aherne and Dunnill (1982).

Cellular Fractionation

Cells grown in 100-mm dishes, after different treatments, were rinsed with PBS and mildly permeabilized by scraping with a rubber policeman in buffer A (150 mM KCl, 2 mM $MgCl_2$, 20 mM HEPES, 10% glycerol, pH 7,2, 1 mM dithiothreitol, 1 mM EGTA, 1 mM EDTA, 1 mM $NaVO_4$, 10 mM NaF, 1 mM phenylmethylsulfonyl fluoride, 10 μg/ml leupeptin, 10 μg/ml aprotinin) supplemented with 0.02% saponin and incubated for 15 min at 4°C to allow the release of cytosolic proteins. The saponin homogenate was then centrifuged at 14,000 $\times$ *g* for 10 min. This centrifugation was sufficient to pellet the saponin-permeabilized cells without loss of membranes. Aliquots (25–50 μg of protein) of soluble and insoluble saponin fraction were processed for electrophoresis and Western blot analysis. Then 8%-SDS-PAGE was performed as described by Laemmli (1970). Electrophoresed proteins were transferred to Immobilon-P transfer membranes (Millipore, Billerica, MA). PKCδ and actin were detected using corresponding primary antibodies diluted in Tris-buffered saline with 0.05% Tween 20 and sheep anti-mouse IgG secondary antibodies (Bio-Rad) conjugated with horseradish peroxidase coupled to the enhanced chemiluminescence system (Amersham Biosciences UK).

Endosomes were prepared essentially as described previously (Grewal *et al*., 2000). Briefly, 4–6 $\times$ 10^7 COS cells were used for each gradient. After removal of the medium, cells were washed two times with cold PBS and scrapped. Pooled cells were centrifuged at 200 $\times$ *g* for 5 min and then gently collected in homogenization buffer (250 mM sucrose, 3 mM imidazol, pH 7.4, and protease inhibitors) and centrifuged at 1500 $\times$ *g* for 10 min. The pellets were homogenized by 20 passages through a 22-gauge needle. Complete homogenization was confirmed under the phase microscope. The homogenate was centrifuged for 15 min at 1000 $\times$ *g*. The postnuclear supernatant (PNS) was brought to a final 40.2% sucrose (wt/vol) concentration by adding 62% sucrose (3 mM imidazol, pH 7.4) to PNS and loaded at the bottom of a SW50.1 centrifugation tubes. Then, 35% sucrose, 25% sucrose, and finally homogenization buffer were poured stepwise on top of the PNS. The gradient was centrifuged for 90 min at 120,000 $\times$ *g*. After centrifugation the endosomal fraction, from 25–35%, corresponding to late and early endosomes were pooled (crude endosomes), and a plasma membrane fraction was collected at the interface of 35/40.2%. The samples were pelleted, and the protein content was measured (Bradford, 1976) using bovine serum albumin as standard.

RESULTS

We already reported the effect of W13 on endocytic compartment morphology and in the blockage of trafficking from this structure, in Madin-Darby canine kidney and COS-1 cells (Apodaca *et al*., 1994; Tebar *et al*., 2002). The use of W13 has been demonstrated to be highly specific for calmodulin, and it does not mimic the effect shown by inhibitors of calmodulin-dependent protein kinases (CaMPKs) or PKC. In the present study, the relationship between calmodulin and PKC was studied to determine their coordinated role in the exit of the EGFR from early endosomes.

Morphology of the Early Endocytic Compartment in Cells Treated with W13 and TPA

As shown previously, in cells treated with W13 (10 μg/ml) almost all EGFR was observed in randomly distributed large endocytic structures (Fig. 1A), compared with control cells (nontreated) and/or cells treated with W12 (our unpublished data). These aberrant endosomes contained early endosomal markers (EEA1 and internalized transferrin or EGF) (Tebar *et al*., 2002).

Because PKC is also actively involved in the signaling and trafficking events leading to the early endocytic compartment, we used TPA to activate PKC in cells previously treated with W13. TPA treatment, alone, already produced enlarged endosomes containing EGFR, but when TPA was combined with W13 an increased/synergistic effect on the size of the early endosomes was observed (Figure 1A). This likely synergistic morphological effect was confirmed by electron microscopy; when ultrathin sections of cells treated with W13 and/or TPA were analyzed by electron microscopy and the average profile area and volume were calculated by morphometric means, a significant increase in the endosomal area and volume after TPA or W13 treatments (5- to 8-fold) and a 20-fold increase in response to the combined application of both TPA and W13, was demonstrated (Table 1).

Table 1. Morphological alterations of early endosomes

	Area (μm^2)	Width (μm)	Height (μm)	β	Volume (μm^3)
Control	0.065	0.333	0.325	1.382	0.023 ± 0.002***
TPA	0.185	0.559	0.471	1.394	0.111 ± 0.009*
W13	0.267	0.575	0.632	1.386	0.192 ± 0.018
W13 + TPA	0.483	0.727	0.853	1.401	0.471 ± 0.049***
W13 + BIM	0.107	0.371	0.374	1.382	0.048 ± 0.008***

Quantification was performed using standard stereological procedures (Weibel, 1979; Aherne and Dunnill, 1982). The electron microscopy images obtained were used to perform the measures of endosomes (endosomal profile area) with the Quantity-One software (Bio-Rad). Data in the table correspond to the mean ± SE of 200 endosomal areas counted from five grids for each experiment and a minimum of 60 different cells. The structures were randomly distributed in the cytoplasmic region of COS-1 cells from grids corresponding to control (cells treated with W12 + EGF) and cells after different treatments (TPA, W13, W13 + TPA, and W13 + BIM), always considering that measured structures were clearly separated from the plasma membrane (see *Material and Methods* for details). Statistical significances of differences between W13 and corresponding treatments were determined using the Student's *t* test with *P < 0.05, ***P < 0.001.

Previously, we have shown that these aberrant endosomes can be loaded with a short pulse of HRP (Apodaca *et al*., 1994) and more recently by immunofluorescence confirmed to contain EGF, transferring, and EEA1 (Tebar *et al*., 2002). The ultrastructure of 7-min HRP-loaded endocytic structures (control and W13-treated cells) was analyzed and showed the typical pleiomorphic early endosomes (our unpublished data).

Also, we have determined whether the activation of PKC (by TPA alone), which causes a similar enlargement of early endosomes (as shown for W13), affected the rate of recycling and/or degradation of EGF; in Figure 1, B and C, it can be observed that no changes in the recycling or degradation rates occurred. These results indicate that calmodulin antagonists as well as PKC activators exert an effect on the morphology of the early endocytic compartment involved in EGFR sorting.

PKC Inhibition Selectively Releases W13 Blockage of Ongoing Recycling from the Early Endocytic Compartment

To elucidate the role of PKC upon the arrest of EGFR trafficking induced in the absence of calmodulin, a broad-spectrum, highly specific PKC inhibitor, BIM, was first used. Immunofluorescence analysis of cells treated with W13 revealed accumulation of EGFR (Figure 2A) and transferrin in early endosome-like vesicles, many of them being enlarged. Whereas incubation with BIM (5 μM) did not alter the staining pattern of the EGFR in control cells, it impaired the formation of W13-enlarged endosomes, either when BIM was incubated before or after W13 (Figure 2A). The same effect was observed with another general PKC inhibitor, staurosporine (100 nM) (our unpublished data).

Electron microscopy showed the morphology of endosomes after W13 and BIM treatments and clearly pointed on

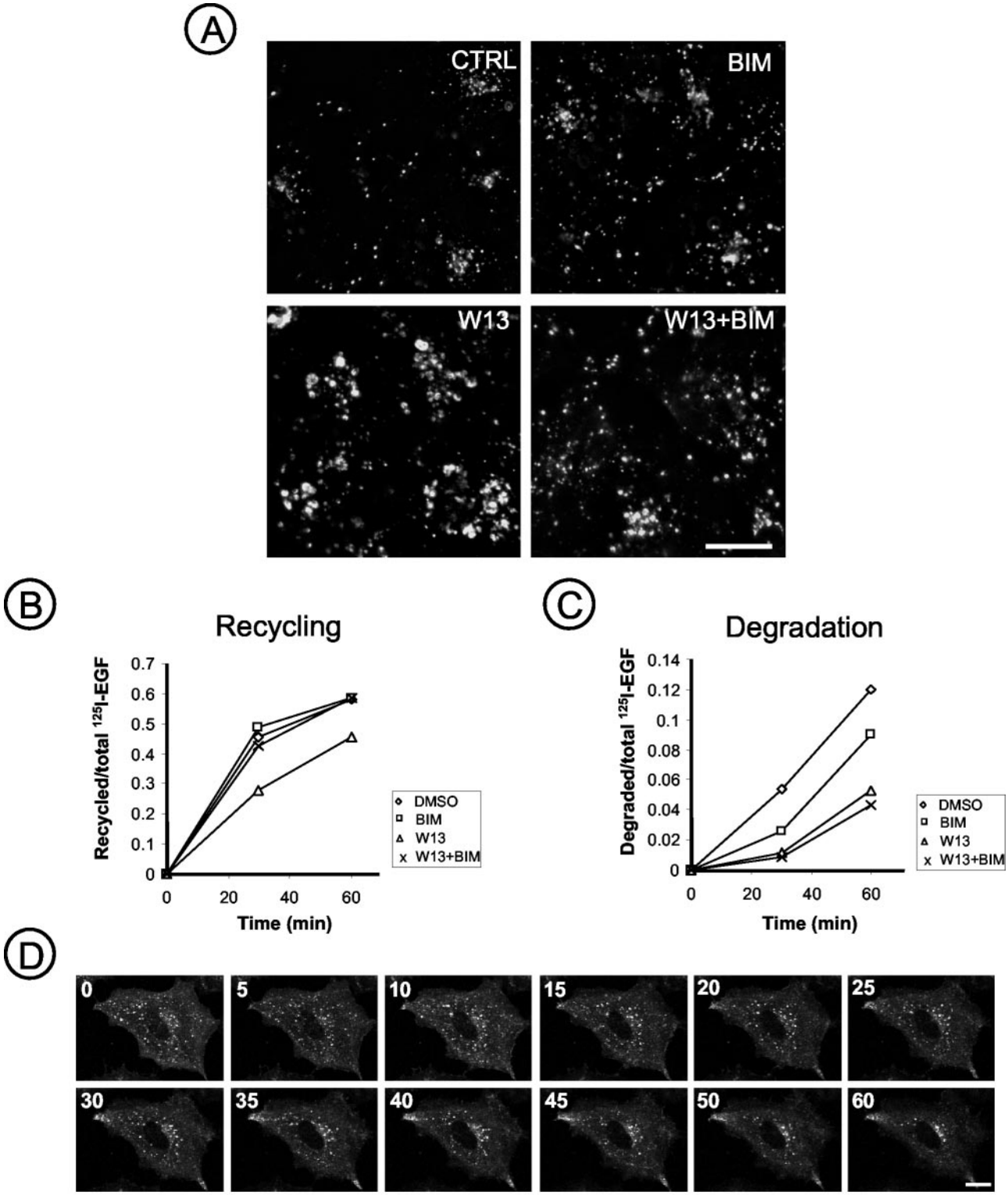

Figure 2. PKC is required for W13-induced endosomal enlargement. BIM restores recycling after W13 but inhibits EGFR degradation. (A) COS-1 cells were incubated for 30 min with W13 (10 μg/ml) and then treated with a general PKC inhibitor (BIM, 5 μM) and EGF-TRITC (200 ng/ml) for 30 min at 37°C. After 7 min of ^{125}I-EGF (5 ng/ml) internalization, COS-1 cells were incubated in the presence of W13 (10 μg/ml) and/or BIM (5 μM) for 1–60 min to measure recycling (B) or degradation (C). Results are shown as the mean of three independent experiments; values did not vary >10% for recycling and 15% in degradation experiments. (D) PAE/EGFR-GFP cells were preincubated with W13 (5 μg/ml) for 60 min at 37°C. After BIM addition, images of GFP labeling were obtained in living cells for 60 min; a selection is shown. Bar (A and E), 10 μm.

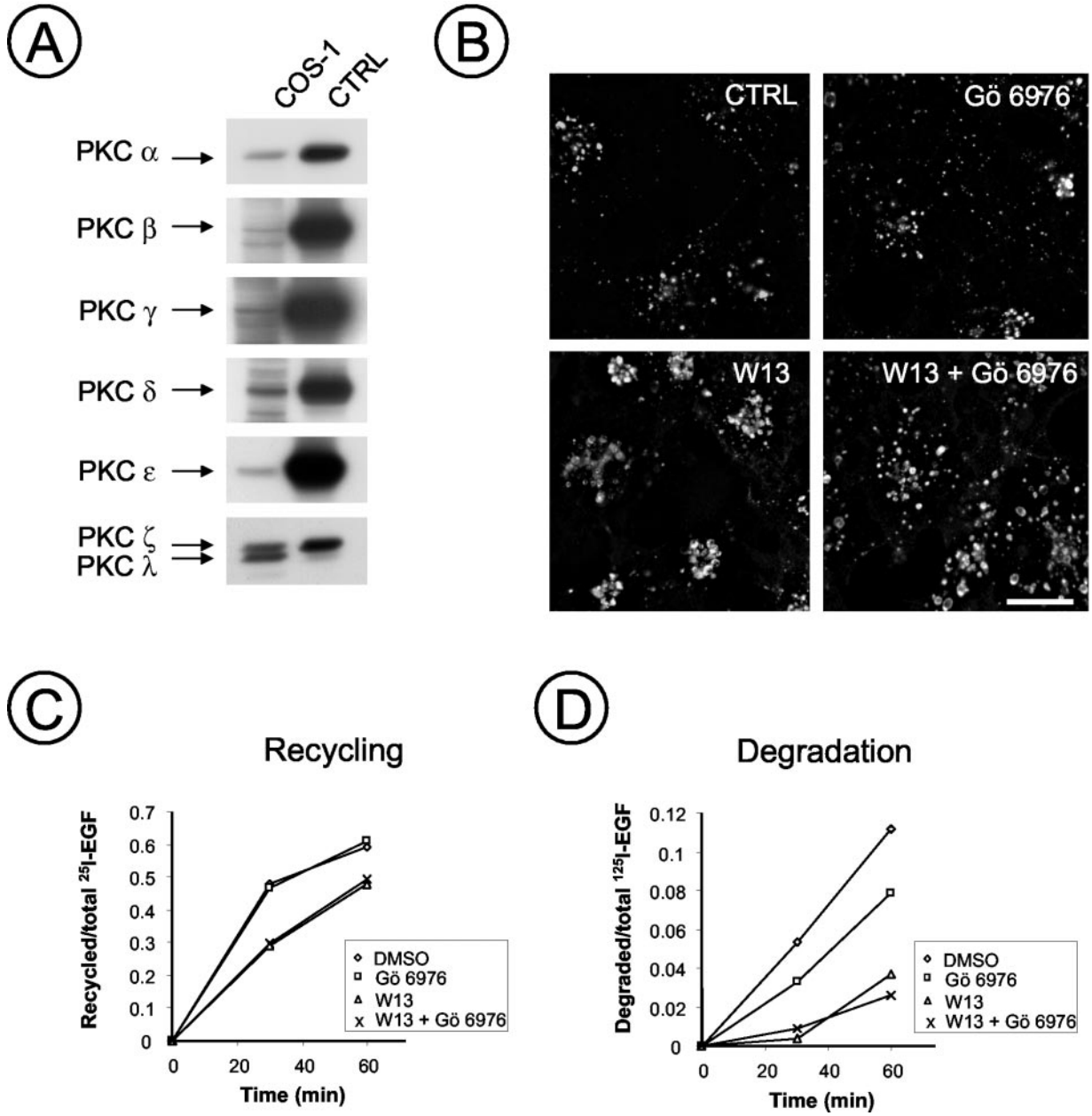

Figure 3. Conventional PKC isoforms are not responsible for the W13 blockage of EGFR trafficking. (A) Equal amounts of protein (50 μg) from COS-1 cell lysates were electrophoresed and the different PKC isoforms (α, β, γ, ϵ, δ, λ, and ζ) detected by Western blotting with the respective specific antibodies. Lysates from rat cerebrum were run in parallel as controls. (B) After 30 min of W13 (10 μg/ml) treatment, COS-1 cells were incubated with a conventional PKC inhibitor (Gö 6976, 1 μM) and EGF (100 ng/ml) for 30 min at 37°C. EGFR was detected with Ab225 and an anti-mouse secondary antibody labeled with Alexa Fluor 546. (C and D) Experiments were performed as explained in Figure 2, C and D, with the Gö 6976 inhibitor instead of BIM. As in Figure 2, values did not vary >10%. Bar (B), 10 μm.

their reduction in area and volume when both reagents were added together (Table 1).

To correlate morphology with the function of these aberrant endosomes, we assessed the effect of BIM (after W13 treatment) on the exit of EGFR from early endosomes to plasma membrane (recycling) or their degradation by using ^{125}I-EGF.

To directly measure recycling rates, cells were loaded with ^{125}I-EGF for 7 min at 37°C, the remaining surface ^{125}I-EGF was removed by mild acid wash and the recycling of ^{125}I-EGF was measured by the appearance of intact ^{125}I-EGF in the medium and at the cell surface, as described previously (Kornilova *et al*., 1996; see *Materials and Methods*). Because the mechanism of recycling is believed to be the same for unoccupied and occupied EGF receptors, we analyzed the effect of W13 in the presence of BIM on the recycling as well as the degradation of ^{125}I-EGF. Recycling of ^{125}I-EGF was inhibited (by 40%) in the presence of W13. On the other hand, degradation of ^{125}I-EGF was completely blocked in cells incubated with W13 (Figure 2, B and C), in agreement with our previous data (Tebar *et al*.2002).

Interestingly, BIM restored the recycling but not the degradation pathway inhibited by W13 (Figure 2, B and C). In

controls using BIM alone to measure the internalization, recycling, and degradation of ^{125}I-EGF, we observed that BIM did not modify either internalization (our unpublished data) or recycling; however, it partially inhibited EGFR degradation rates. This was confirmed by the analysis in vivo in PAE cells stably expressing GFP-EGFR, which showed that addition of BIM after W13 restored regular EGFR trafficking to the perinuclear, Golgi-lysosomal area (Figure 2D). Together, these results indicate that the effect of calmodulin on EGFR trafficking/sorting at the level of early endosomes is significantly dependent on PKC.

Dissection of the Role of PKC Isoforms in the Regulation of Recycling from the Early Endocytic Compartment: PKCδ Is Involved in the Exit from Endosomes

The presence of different PKC isoforms (α, β, γ, δ, ϵ, ζ, and λ) in cell lysates of COS-1 cells was demonstrated by Western blotting with specific antibodies (Figure 3A). Because these different members of the PKC superfamily have been shown to be involved in a variety of physiological processes, we wished to determine which of these isoforms is specifically required in the early endocytic compartment for sorting of the EGFR.

To ascertain the identity of the PKC isoform implicated in the inhibition of EGFR trafficking/sorting from early endosomes in the absence of calmodulin, Gö6976, a specific inhibitor of conventional PKCs (cPKC; α, β, and γ) as well as for the novel PKC-μ(PKD) was tested.

COS-1 cells treated with W13 revealed accumulation of EGFR (Figure 3B) in enlarged early endosomes. The addition of Gö 6976 (1 μM) did not modify the staining pattern of EGFR in control cells, nor did it impair the formation of W13-enlarged endosomes (Figure 3B). Quantitative analyses were performed to confirm the immunofluorescence data: addition of Gö 6976 did not affect the recycling process, in the presence or absence of W13; nevertheless, it diminished ^{125}I-EGFdegradation by 30% in control cells (Figure 3, C and D). These results showed that neither conventional PKC isoforms nor PKCμ are implicated in the effect of W13.

Next, we focused on the atypical PKC isoforms (aPKC, λ and ζ), which do not respond to either DAG (diacylglycerol) or calcium, although they still require PS (phosphatidylserine) as cofactor. Atypical PKC isoforms have been involved in vesicular transport (Sanchez *et al*., 1998). COS-1 cells, transiently expressing dominant-negative forms of PKCλ or PKCζ were incubated with W13 and then EGF. Figure 4 shows that neither PKCλ nor PKCζ dominant-negative expression interfered with W13 effects.

Finally, we studied the novel PKC subfamily. nPKC isoforms are activated by DAG and require phosphatidilserine as a cofactor, but are Ca^{2+} independent. This subfamily is composed of ϵ, δ, η, and θ. Figure 5 shows the effect of expression of a dominant-negative form of PKCϵ in COS-1 cells treated with W13; no effect on the distribution of EGFR could be observed in those cells expressing the dominant-negative form (Figure 5A). However, its implication cannot be ruled out because overexpression of this mutant caused, in some cases, a considerable decrease in EGFR expression and also altered EGFR trafficking (our unpublished data). Indeed, the EGFR was mislocalized in small vesicle-like, structures randomly distributed in the cytosol.

Next, we used rottlerin, a specific inhibitor of the PKCδ isoform (Kikkawa *et al*., 2002). It has been demonstrated that at low concentration (3–6 μM) rottlerin only inhibits the PKCδ isoform. At high concentration (30–50 μM), it can inhibit the cPKCs and at higher concentration (100 μM) PKCϵ, η, and ζ (Gschwendt *et al*., 1994). Rottlerin also can be used to discriminate PKCϵ. Starved COS-1 cells, preincubated with W13 to allow the enlarged endosome formation, were incubated with rottlerin (1–5 μM) and EGF (100 nM) for 30 min at 37°C. The EGFR distribution was assessed using an anti-EGFR antibody (Ab225) and the corresponding secondary labeled with Cy3. Although rottlerin did not modify the subcellular localization of EGFR in control cells (our unpublished data), it inhibited the effect produced by W13 (Figure 5B). Because at low concentration (2 μM) rottlerin also inhibits PRAK (Davies *et al*., 2000), a p38 inhibitor (SB 203580) was used to rule out PRAK (p38-regulated or -activated kinase) involvement; no interference was observed with the W13 response (our unpublished data).

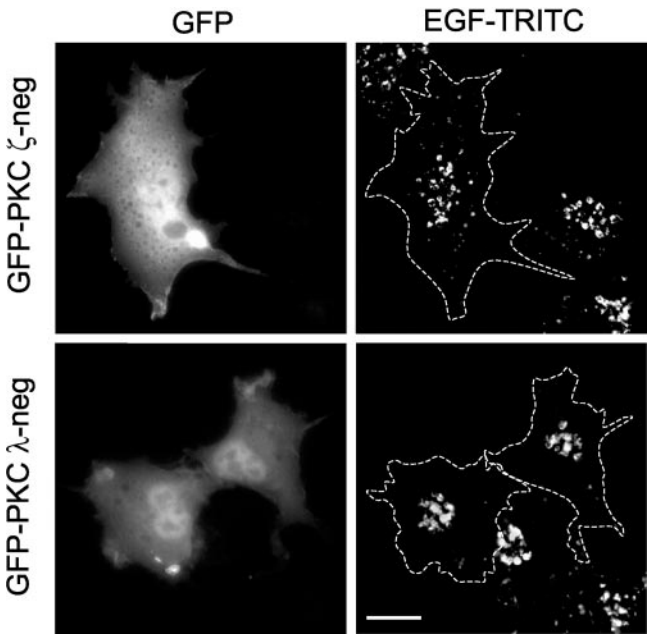

Figure 4. Expression of dominant-negative forms of atypical PKC does not interfere with W13 effect. COS-1 cells transiently expressing GFP-dominant-negative aPKCλ or ζ were incubated for 60 min with W13 (10 μg/ml) and the final 20 min with EGF-TRITC (200 ng/ml) at 37°C. Atypical dominant-negatives and EGF images were acquired through the GFP and TRITC channel, respectively. Bar, 10 μm.

To confirm the effect of rottlerin, as shown previously for BIM, a quantitative assay to measure the recycling and degradation of EGF by using ^{125}I-EGF was performed. Rottlerin almost completely restored recycling inhibited by W13 (Figure 5C) but did not recover EGF degradation (Figure 5D). As with other inhibitors tested, rottlerin also inhibited EGF degradation in control cells, in this case the effect being more pronounced (45%).

In agreement with the result exposed with rottlerin, Figure 6A shows the effect of expression of a dominant-negative PKCδ in COS-1 cells treated with W13; cells expressing the dominant-negative form did not reveal the accumulation of EGF-TRITC or the formation of enlarged early endocytic structures labeled with EEA1. The effect of rottlerin upon the reversion of the W13 was observed in a large number of cells compared with the dominant-negative that was detected in $\approx$60% of the transfected cells.

Finally, to investigate whether PKCδ had a direct role to play in the recycling of EGF from the early endosomes, in the absence of calmodulin, two different siRNAs oligonucle-

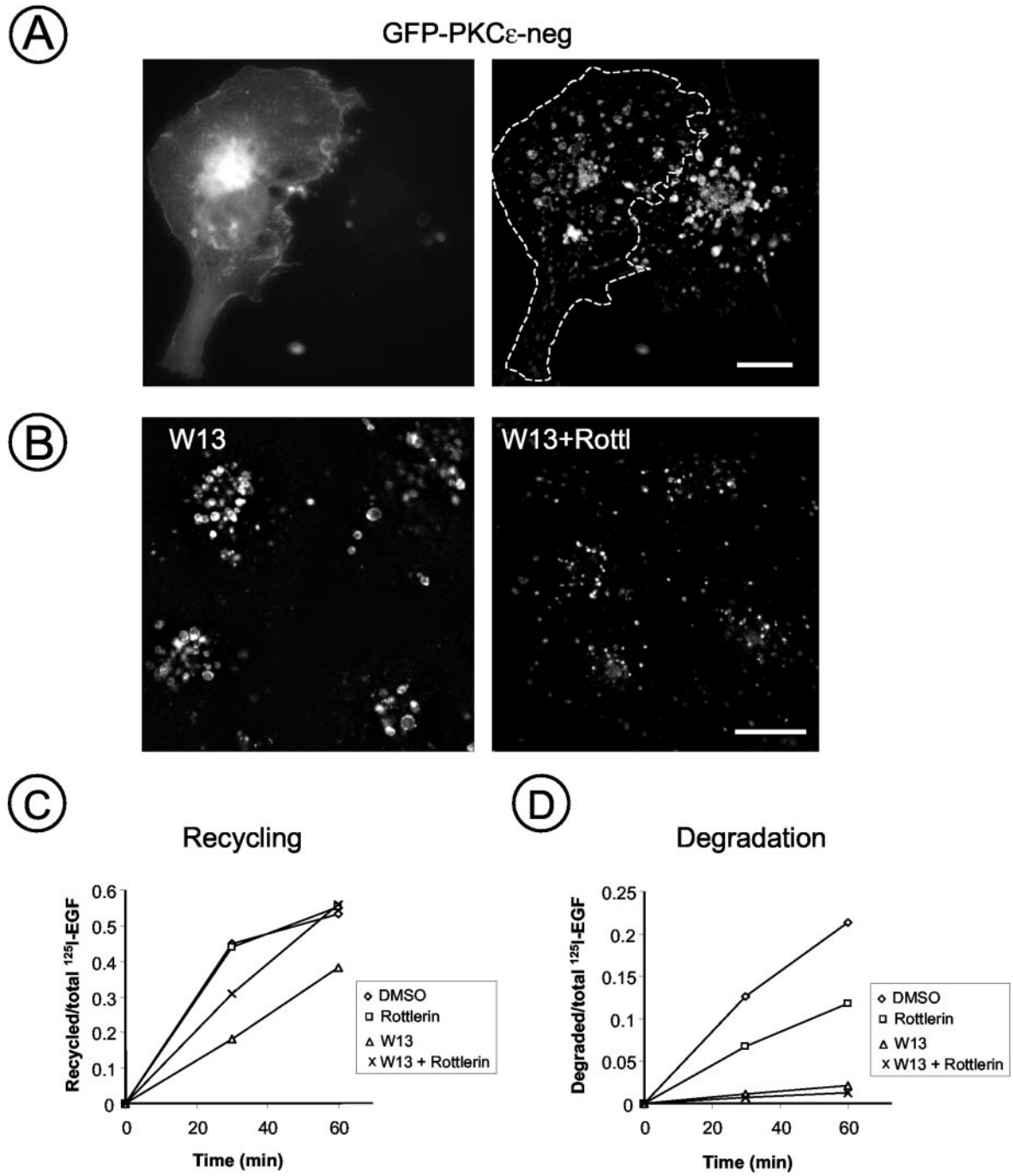

Figure 5. PKCδ, but not PKCε, is necessary for W13-enlarged endosomes. (A) COS-1 cells transiently expressing GFP-dominant-negative nPKCε were incubated for 45 min with W13 (10 μg/ml), and afterward, 20 min with EGF-TRITC (200 ng/ml) at 37°C. (B) After a 30-min pretreatment with W13 (10 μg/ml), COS-1 cells were incubated with a PKCδ inhibitor (rottlerin, 5 μM) and EGF (100 ng/ml) for 30 min at 37°C. EGFR was detected with Ab225 and an anti-mouse secondary antibody labeled with Alexa Fluor 488. Bar, 10 μm. (C and D) After 7 min of ^{125}I-EGF (5 ng/ml) internalization, COS-1 cells were incubated in the presence of W13 (10 μg/ml) and/or rottlerin (5 μM), for 1–60 min to measure recycling (C) or degradation (D). Results are shown as the mean of three independent experiments (triplicates) and values did not vary >10%.

otides complementary to two regions of human PKCδ were transfected into HeLa cells (siRNA2 was used in Figure 6). The expression of PKCδ was significantly reduced (≈85%) by siRNA2 after 72 h (Figure 6B). Down-modulation of PKCδ was specific and the amounts of other early endosomal proteins such as EEA1 or Rab5, remained unchanged (Figure 6B).

We then measured the recycling and degradation of internalized ^{125}I-EGF after siRNA-mediated down-regulation of PKCδ, in HeLa cells. Figure 6C shows the percentage of

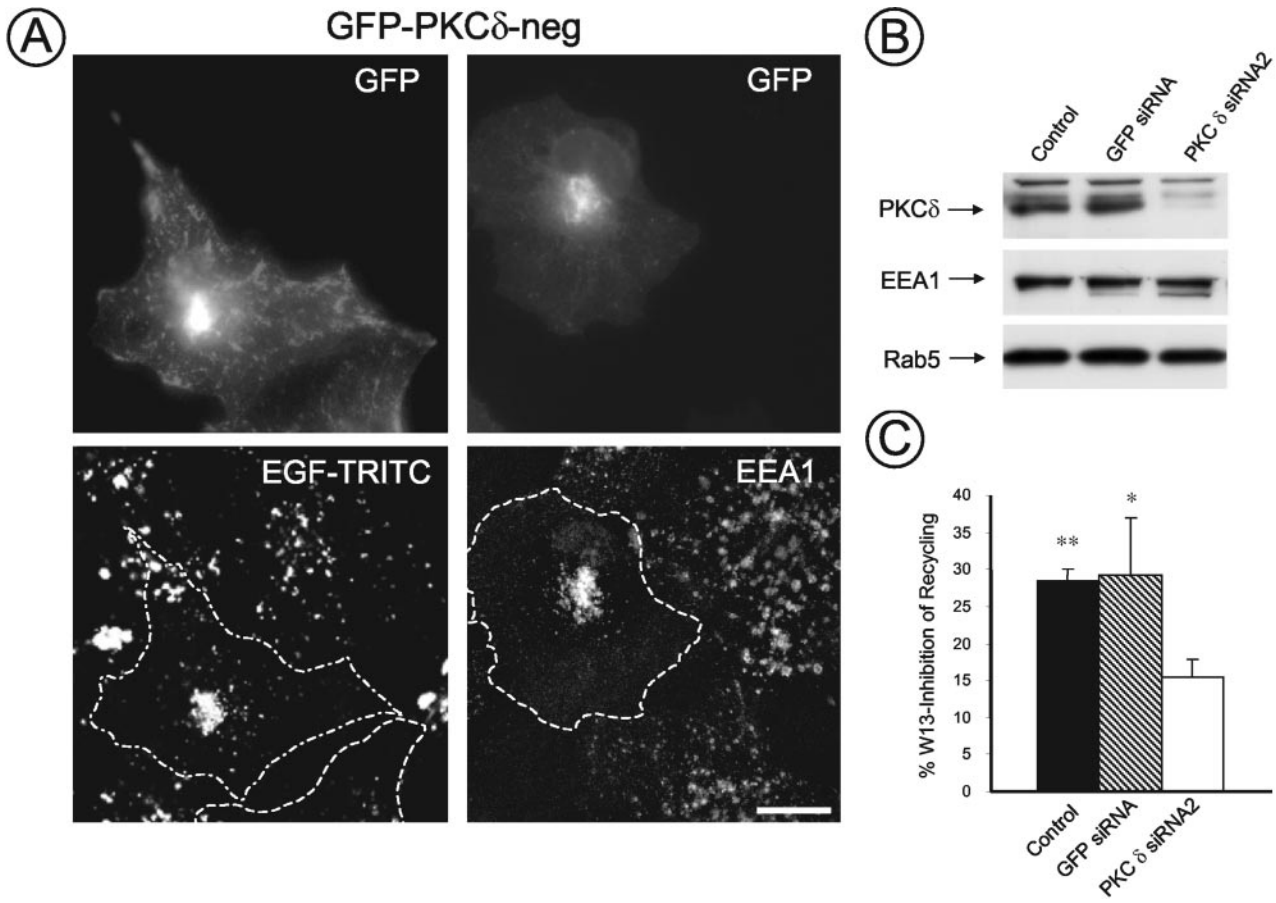

Figure 6. PKCδ down-modulation releases W13 blockage of recycling. (A) COS-1 cells transiently expressing GFP-dominant-negative PKCδ were incubated for 45 min with W13 (10 μg/ml), and afterward, 20 min with EGF-TRITC (200 ng/ml) at 37°C. A also shows a transfected cell immunolabeled with anti-EEA1. (B) HeLa cells were transfected for 72 h with siRNA2 or GFPsiRNA and analyzed by SDS-PAGE and Western blotting, by using antibodies against PKCδ, EEA1, and Rab5. (C) HeLa cells were incubated in the presence of W13 (10 μg/ml), for 30 min; the percentage of inhibition of recycling in siRNA-transfected is shown. Data in the histograms shows a mean of two independent experiments. Statistical significances of differences between PKCδ siRNA and the corresponding controls were determined using the Student's *t* test. *$P < 0.05$, **$P < 0.01$. Control, no transfection.

inhibition of recycling in cells treated with W13 for 30 min after 72 h of siRNA2 transfection; down modulated of PKCδ involved a release of recycling of ≈50%. On the other hand (as for rottlerin; Figure 5D), in siRNA2-transfected untreated cells degradation was inhibited by 35% (our unpublished data).

Cytosolic and particulate fractions were isolated from COS-1 cells, and the amount of PKCδ after different treatments was analyzed by Western blotting. PKCδ translocates from the cytosol to the particulate fraction after TPA activation (20 min) (Figure 7A). In the presence of W13, a significant increase in PKCδ was detected in this particulate (membrane-rich), compared with control untreated samples. However, because the specific cellular location is important, we have isolated endosomes and plasma membrane from COS-1 cells after different treatments. Figure 7B shows that total and the active PKCδ, determined using the antibody that recognize the phosphorylation at the serine-643 (Li *et al*., 1997; Stempka *et al*., 1999), were present in endosomes (enriched in Rab5) independently of the treatment.

Role of Calmodulin and PKCδ in Tubulation from the Early Endosomes

To understand the molecular mechanism by which the concerted action of calmodulin and PKCδ regulate budding (to the recycling pathway) from the early endosomal compartment, we investigated the membrane tubulation, a process that has been directly involved in the endosomal recycling (Lippincott-Schwartz *et al*., 1991). It has been suggested that calmodulin is a regulator of membrane tubulation and therefore is capable of influencing the morphology and function of several organelles (de Figueiredo and Brown, 1995).

BFA promotes tubulation from Golgi cisternae and also from early endosomes (Wood and Brown, 1992). W13 was shown to inhibit BFA-mediated endosome tubulation (de Figueiredo and Brown, 1995). Interestingly, this effect (inhibition of tubulation) was completely reversed by the addition of rottlerin, as shown using transferrin-TRITC, in COS-1 cells (Figure 8A); BFA-mediated endosome tubulation also was observed in TPA-stimulated cells as well as after BFA + rottlerin treatment (i.e., stimulation of PKC by TPA did not block the BFA-induced tubulation in endosomes). The same can be observed for EGFR by using GFP-EGFR in PAE cells (Figure 8B).

Finally, we studied whether rottlerin was able to restore the traffic to late endosomal compartments (despite its inhibition of EGF degradation). To this end, transport of dextran-TRITC was followed along the endocytic route.

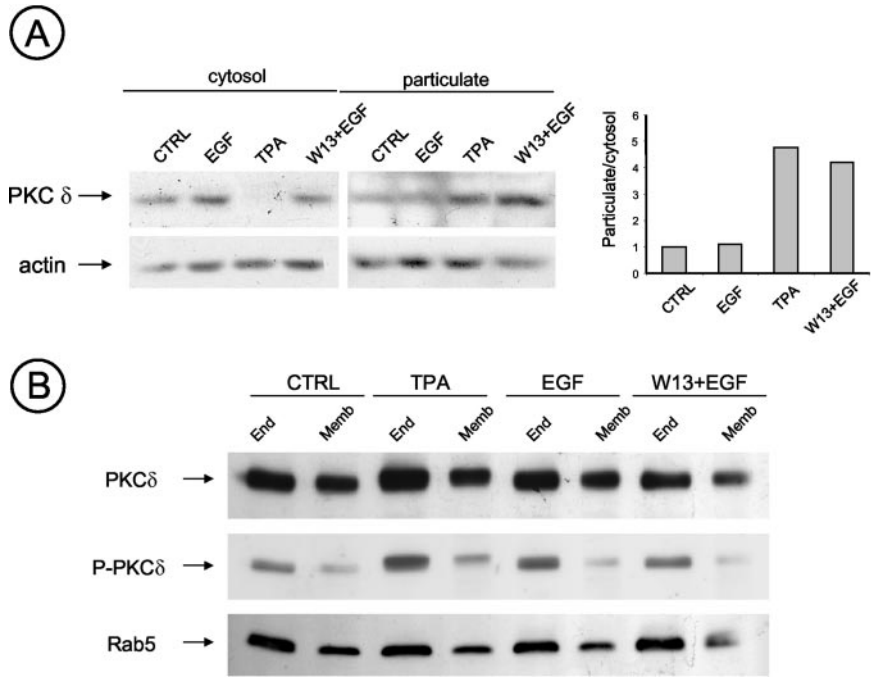

Figure 7. Active PKCδ in the endocytic compartment. (A) Starved COS-1 cells were treated with TPA (100 nM), EGF (100 ng/ml), and/or W13 (10 μg/ml). The saponin soluble (cytosolic) and insoluble (particulate) fractions were obtained as described in *Materials and Methods* and resolved by SDS-PAGE. PKCδ and actin were detected by Western blotting with specific monoclonal antibodies and a representative experiment is shown. Densitometric analysis of the PKCδ chemiluminescence intensity was corrected by actin signal and the histogram shows the ratio of particulate to cytosolic labeling of three independent experiments. (B) Western blot analysis of total and active PKCδ (P-S643-PKCδ) in isolated endosomes (End) and plasma membrane (Memb) fractions from COS-1 cells after indicated treatments. Rab5 indicated the enrichment of early endosomes in this crude endosomal fraction.

COS-1 cells were preincubated with W13 (for 45 min) and loaded with dextran-TRITC for 15 min to label the enlarged endosomes formed. Subsequently, rottlerin was applied and the time course of dextran-TRITC subcellular localization was studied. Rottlerin partially restored the traffic of dextran from the aberrant endosomes, where it was trapped, to the perinuclear Golgi area (Figure 8C). Some of these perinuclear-labeled structures colocalized with LBPA-positive endosomes (LBPA is a specific late endosomal marker) (Figure 8D). Together, these results clearly show that PKCδ and calmodulin coordinately regulate budding/exit from early endosomes.

DISCUSSION

Calmodulin antagonists have been previously shown to exert a severe effect on endocytic trafficking at the level of early endosomes (Tebar *et al*., 2002). Now, in this study we have demonstrated that, in the absence of functional calmodulin, PKCδ is responsible to inhibit the recycling of the EGFR from the early endocytic compartment.

Calmodulin antagonists have proved to be very useful to study its role in different physiological processes, including membrane trafficking. Other groups and ourselves, have studied the involvement of calmodulin in the various processes of membrane traffic such as: endocytosis (Apodaca *et al*., 1994; Llorente *et al*., 1996; Della: Rocca *et al*., 1999), recycling (Apodaca *et al*., 1994; de Figueiredo and Brown, 1995; Huber *et al*., 2000), transcytosis (Apodaca *et al*., 1994; Hunziker, 1994) and at the completion of docking and the late steps of vacuole fusion (Peters and Mayer, 1998) or in endosome fusion (Lawe *et al*., 2003).

In general, there is an agreement that the morphology of the early endocytic compartment is modified by the calmodulin antagonists (Apodaca *et al*., 1994; de Figueiredo and Brown, 1995; Llorente *et al*., 1996; Tebar *et al*., 2002). It was proposed that calmodulin antagonists could inhibit the transport of receptors out of endosomes by inhibiting the formation of the tubular recycling structures (de Figueiredo and Brown, 1995).

However, the mechanisms of W13 inhibition of endosomal function remain to be investigated and several possibilities can be considered. First, the effects of W13 could be mediated by components of the fusion-budding machinery, such as annexins, EEA1, synaptobrevin (vesicle-associated membrane protein 2) or phosphoinositide 3-kinase, which are either Ca^{2+} or calmodulin binding proteins (Mayorga *et al*., 1994; Mu *et al*., 1995; Colombo *et al*., 1997; Quetglas *et al*., 2000; Burgoyne and Clague, 2003; Lawe *et al*., 2003). Second, calmodulin may control the endosomal apparatus via the actin cytoskeleton, through GTPases of the Rho or ARF subfamilies (e.g., Rac and ARF6) (Hall, 1994; Schmidt and Hall, 1998; Ridley, 2001) or through different actin-associated calmodulin binding proteins (e.g., myr4) (Huber *et al*., 2000). In addition, the effect of calmodulin antagonists on the lipidic environment should be taken into account, as in the regulation of a lipid binding domain in the v-SNARE synaptobrevin, for vesicular fusion/fission events (De Haro *et al*., 2003), or in the perturbation of polyphosphoinositide metabolism, which might be important in the organization of the actin cytoskeleton via phosphatidylinositol (4,5)-biphosphate synthesis (Desrivieres *et al*., 2002). Furthermore, changes in lipid composition, caused by alterations in the protein–protein interactions as a consequence of calmodulin depletion, may induce the formation of membrane domains that can recruit other molecules, such as annexins or PKC, which eventually might contribute to the functioning of endocytic structures. Finally, it has been recently shown that calmodulin seems to be required to maintain a stable interactions of EEA1 with the endosomal membrane and therefore be essential for the fusion machinery (Lawe *et al*., 2003).

PKC and the Endocytic Compartment

In addition to the known role of PKC as a mediator of transmembrane signaling initiated at the plasma membrane, there is now significant evidence to suggest that sustained PKC activity regulates a variety of long-term cellular pro-

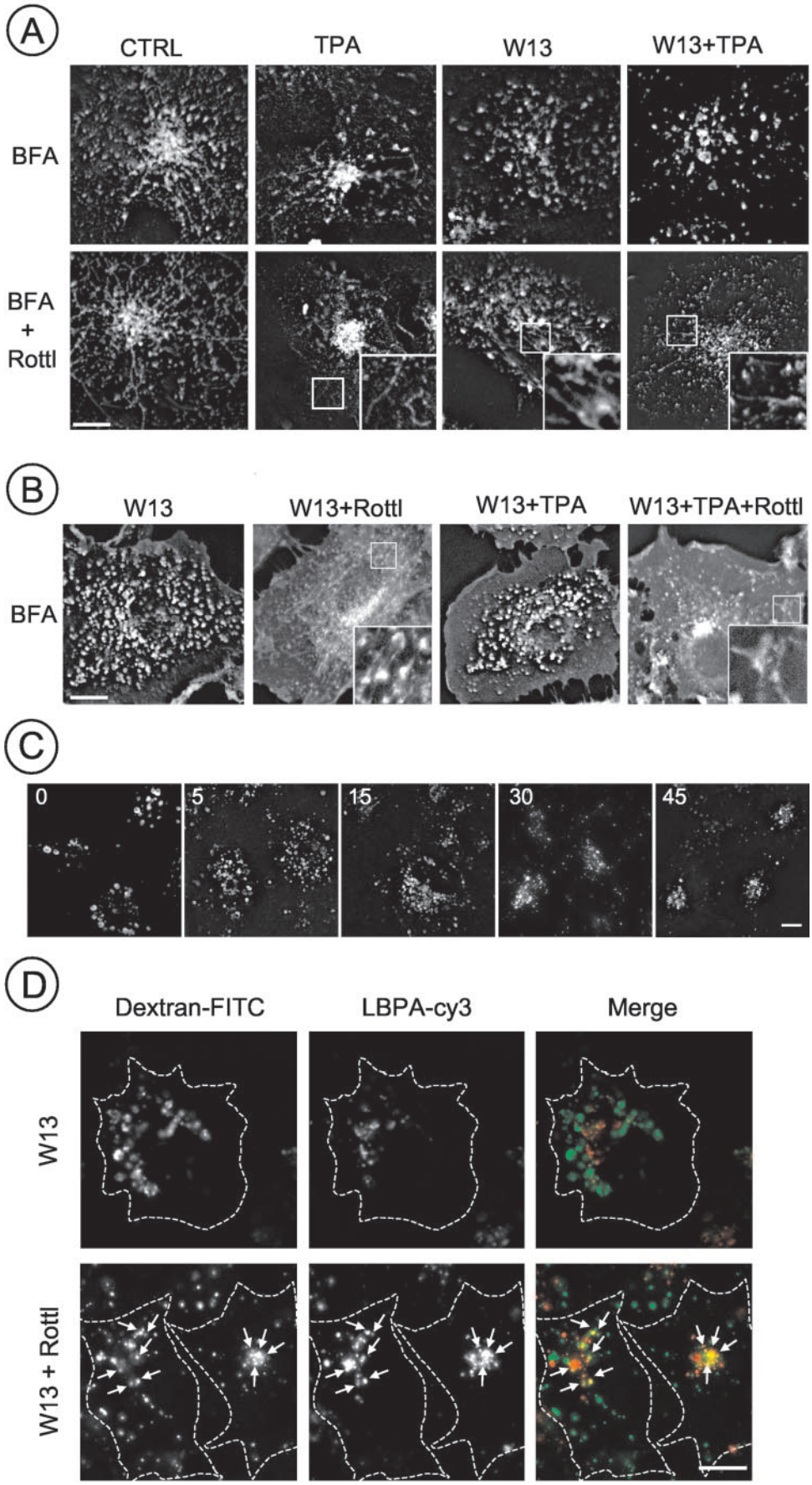

Figure 8. In the absence of calmodulin, PKCδ inhibits tubulation and late endosomal transport from early endosomes. (A and B) The effect of rottlerin on BFA-tubulation, in early endosomes, was examined. (A) COS-1 cells were preincubated for 45 min with W13 (10 μg/ml) and/or 15 min with TPA (100 nM). After 15 min with transferrin-TRITC, cells were incubated with BFA (10 μg/ml) and/or rottlerin (5 μM) for 10 min and fixed. Images were acquired through the Red filter channel. (B) PAE/GFP-EGFR cells were treated as explained in A, and images were acquired through the GFP filter channel. Insets, high magnification of the selected white rectangle area. Insets show a detail of tubulation after rottlerin treatment. (C) COS-1 cells were incubated with W13 (10 μg/ml) and dextran-TRITC (5 mg/ml) for 60 and 15 min, respectively. The effect of rottlerin (5 μM) on subcellular localization of dextran was visualized at the indicated times in fixed cells. (D) Double labeling of dextran-FITC and anti-LBPA (with the corresponding secondary anti-IgG-cy3) to visualize the late endocytic structures loaded with dextran-FITC after W13 and rottlerin (45 min) treatment. Arrows show the colocalization. Bar, 10 μm.

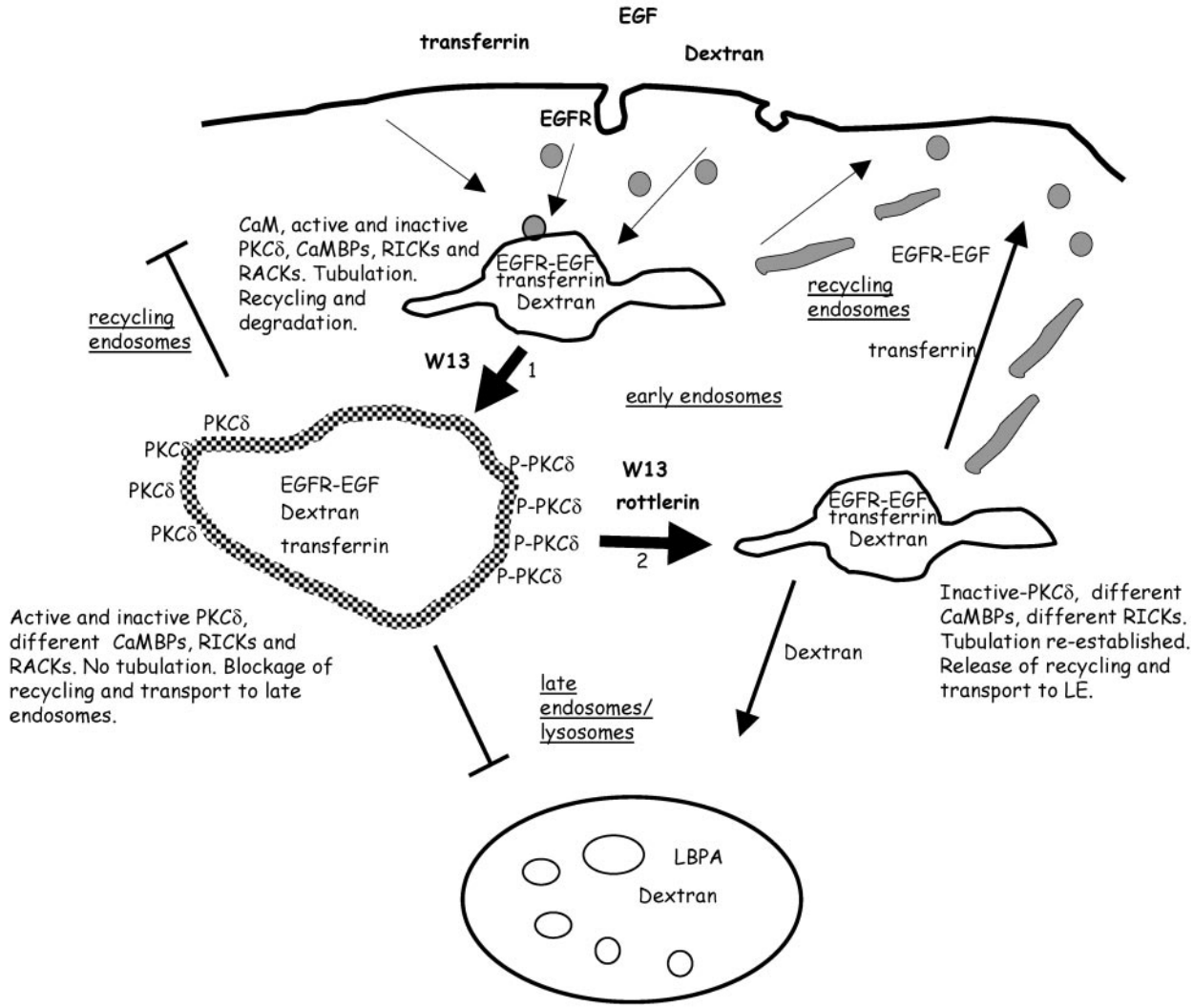

Figure 9. Schematic representation of calmodulin-PKCδ–regulated EGFR trafficking along the early endocytic compartment. Briefly, 1) W13 treatment (depletion of calmodulin) involves a rapid and reversible morphological alteration in early endosomes containing activated-PKCδ plus other proteins (and/or protein complexes: CaMBPs, RICKs, and RACKs) with the inhibition of tubulation and the blockage of recycling of EGFR and transferrin and the transport to late endosomes, i.e., the exit from this endocytic compartment. 2) However, in cells depleted of calmodulin and with inactive PKCδ (W13 plus rottlerin or expression of dominant-negative PKCδ), the tubulation was reestablished and the recycling and the fluid phase transport were restored. EE, early endosome; LE, late endosome.

cesses. Nevertheless, subcellular location and translocation are of particular significance; treatment of cells with a variety of PKC agonists/phorbol esters led to localization of PKC to the Golgi complex, nuclear envelope, mitochondria, and/or the cytoskeleton (Saito *et al*., 2002). Besides, the endosomal compartments (early and late endosomes as well as lysosomes) are becoming emerging targets for different isoforms of PKC (Cardone, Mochly-Rosen, and Enrich, unpublished data; Prevostel *et al*., 2000; Le *et al*., 2002).

At the plasma membrane, PKC-induced phosphorylation of the EGFR at Thr654 is sufficient to direct internalized receptors to the recycling endosomes (Bao *et al*., 2000). However, it is not known whether PKCδ phosphorylates the threonine 654 of EGFR; the activity of a purified PKC isozyme mixture (α, β, γ, ϵ, and ζ) can be inhibited by the substrate peptide RKRCLRRL, that is part of the calmodulin binding domain of EGFR in which T (is threonine 654) was change by C (Ward *et al*., 1995, 1996). This could be extrapolated as if they could act upon the Thr654 of EGFR, although this has not been confirmed in in vivo or for the PKCδ isoform. However, although PKCα has been implicated in the delivery to early endosomes via a caveolae-mediated process (Prevostel *et al*., 2000) or in the regulation of endocytosis and recycling of E-selectin (Le *et al*., 2002), little is known about the specific roles of PKC in regulating recycling pathway.

Biochemical and immunocytochemical studies have indicated that the biological activity of PKC is intimately regulated by its subcellular localization; especially, those cPKC and less nPKC that translocate to the plasma membrane in response to DAG and tumor-promoting phorbol esters. Phosphorylation and autophosphorylation of PKC are critical for the regulation of its cellular distribution or enzymatic activity and for the dynamic cellular trafficking, most probably by enhancing reverse translocation (Ohmori *et al*., 1998; Feng *et al*., 2000; Iwabu *et al*., 2004).

Becker and Hanunn (2003) recently demonstrated a coincident cPKC translocation into a juxtanuclear compartment

with a sequestration of membrane-recycling components, this occurred in a PKC kinase activity-dependent manner, suggesting a role for cPKC in the endosome recycling compartment. This recycling compartment was Rab11 positive and contained transferrin.

Calmodulin and Anchoring Proteins for PKCδ Can Be Involved in the Regulation of Protein–Protein Interactions and the Exit from the Early Endocytic Compartment

In the present study, we have shown that, in the absence of calmodulin, active PKCδ blocks the exit of EGFR toward the recycling pathway. It is believed that some membrane receptors concentrate into endosome tubular extensions, before recycling back to the plasma membrane (Geuze *et al*., 1984). Consequently, the exit/budding from a donor membrane compartment depends on tubulation, and it has been shown that inhibition of this process blocks recycling (de Figueiredo *et al*., 2001, and references therein). Thus, although it is a rather general process, occurring at the Golgi, the endoplasmic reticulum and from endosomal structures, the molecular machinery and the underlying mechanism(s) is not known. Tubule formation from endosomes requires, at least, cytosolic Ca^{2+}-independent phopholipase A_2 activity (de Figueiredo *et al*., 2001) and myr4, an actin-based mechanoenzyme, which binds calmodulin and is involved in recycling endosomes (Huber *et al*., 2000).

The regulation by calmodulin is extremely fine and the local arrangement of protein complexes in each intracellular compartment is central for the overall regulatory process. It has been recently demonstrated (for Ca^{2+} channels) that crucial to calmodulin function is the number of (calmodulin) molecules regulating a particular calmodulin binding protein (CaMBP) (Mori *et al*., 2004).

Finally, it should be consider the complexity of the regulation of PKC by lipids and proteins that may establish spatiotemporal interactions in a particular location (i.e., the endocytic compartment); both inactive and active PKC isoenzymes are localized to specific anchoring molecules: RACK, for receptor activated C-kinase and RICKs, receptors for inactive C-kinase isoenzymes. It seems that each isoenzyme may have several different proteins that anchor it to different subcellular sites in the inactive (RICKs) or activated states (RACKs). It is likely that the unique cellular functions of PKCs are determined by the binding of isoenzymes to specific anchoring molecules in proximity to particular subsets of substrates and away from others (Mochly-Rosen and Gordon, 1998).

Therefore, the model that is proposed from the data is summarized in Figure 9. In early endosomes from control cells, calmodulin, activated PKCδ, CaMBPs, RICKs, and RACKs are present; then, depletion of calmodulin (+W13) prevents tubulation and promotes the enlargement of early endosomes and the blockage of intracellular trafficking (along the recycling and degradation pathways), activated PKCδ is present in these aberrant early endosomes. In cells depleted of calmodulin, but with the PKCδ inactive, the recycling of EGFR and fluid phase transport to the late endosomes was significantly restored; this can be in part due to alternative interactions with RICKs.

Together, calmodulin-PKCδ cross talk seems to be a critical event for the exit from the early endocytic compartment but also could be a more general mechanism controlling other intracellular trafficking pathways. In addition, we have provided evidence that PKCδ can be considered as part of the molecular machinery in processes of membrane tubulation such as in endosome recycling.

ACKNOWLEDGMENTS

This work was supported by grants G03/015 from Ministerio de Sanidad y Consumo and BMC2003-04754 and GEN2003-20662 from Ministerio de Educación y Ciencia to C.E. and BMC2003-09496 to F.T. A.L. is grateful to Agència de Gestió d'Ajuts Universitaris i de Recerca. (Generalitat de Catalunya) for a short-term fellowship. We thank to Dr. Jorge Moscat (Centro de Biología Molecular, Severo Ochoa, Madrid, Spain) and Dr. C. Larsson (Lund University) for providing the different cDNAs encoding the dominant-negatives of PKC isoforms. Also, we are thankful to Serveis Científic i Tècnics de la Universitat de Barcelona for assistance in the confocal and electron microscopy and to Dr. Joan Serratosa (Consejo Superior de Investigaciones Cientificas, Barcelona, Spain) for a helpful assistance in the stereological analysis. A.S. is supported by grants from National Cancer Institute and National Institute on Drug Abuse. M.C. Serveis Científic i Técnics, Universitat de Barcelona, is grateful to grant PI021125 from Ministerio de Sanidad y consumo. J.M. is supported by a predoctoral fellowship from Institut d'Investigacions Biomèdiques, August Pi i Sunyer. (Barcelona, Spain).

REFERENCES

Aballay, A., Stahl, P.D., and Mayorga, L.S. (1999). Phorbol ester promotes endocytosis by activating a factor involved in endosome fusion. J. Cell Sci. *112*, 2549–2557.

Aherne, W.A., and Dunnill, M.S. (1982) Morphometry, ch. 7, London: Edward Arnold Publishers Ltd. London, 82.

Anderson, C.M., and Olefsky, J.M. (1991). Phorbol ester-mediated protein kinase C interaction with wild type and COOH-terminal truncated insulin receptors. J. Biol. Chem. *266*, 21760–21764.

Apodaca, G., Enrich, C., and Mostov, K.E. (1994). The calmodulin antagonist, W-13, alters transcytosis, recycling, and the morphology of the endocytic pathway in Madin-Darby canine kidney cells. J. Biol. Chem. *269*, 19005–19013.

Bao, J., Alroy, I., Waterman, H., Schejter, E.D., Brodie, C.H., Gruenberg, J., and Yarden, Y. (2000). Threonine phosphorylation diverts internalized epidermal growth factor receptors from degradative pathway to the recycling endosome. J. Biol. Chem. *275*, 26178–26186.

Becker, K.P., and Hannun, Y.A. (2003). cPKC-dependent sequestration of membrane-recycling components in a subset of recycling endosomes. J. Biol. Chem. *278*, 52747–52754.

Bradford, M.M. (1976). A rapid and sensitive method for the quantitation of microgram quantities of protein. Anal. Biochem. *72*, 248–254.

Burgoyne, R.D., and Clague, M.J. (2003). Calcium and calmodulin in membrane fusion. Biochim. Biophys. Acta *1641*, 137–143.

Carter, R.E., and Sorkin, A. (1998). Endocytosis of functional epidermal growth factor receptor-green fluorescent protein chimera. J. Biol. Chem. *273*, 35000–35007.

Colombo, M.I., Beron, W., and Stahl, P.D. (1997). Calmodulin regulates endosome fusion. J. Biol. Chem. *272*, 7707–7712.

Chen, Y.-W., Lang, M.C., and Wade, W.F. (2004). Protein kinase C-α and -δ are required for Fcα R (CD89) trafficking to MHC class II compartments and Fcα R-mediated antigen presentation. Traffic *5*, 577–594.

Davies, S.P., Reddy, H., Caivano, M., and Cohen, P. (2000). Specificity and mechanism of action of some commonly used protein kinase inhibitors. Biochem. J. *351*, 95–105.

de Figueiredo, P., and Brown, W.J. (1995). A role for calmodulin in organelle membrane tubulation. Mol. Biol. Cell *6*, 871–887.

de Figueiredo, P., Doody, A., Polizotto, R.S., Drecktrah, D., Wood, S., Banta, M., Strang, M.S., and Brown, W.J. (2001). Inhibition of transferrin recycling and endosome tubulation by phospholipase A2 antagonists. J. Biol. Chem. *276*, 47361–47370.

De Haro, L., Quetglas, S., Iborra, C., Leveque, C., and Seagar, M. (2003). Calmodulin-dependent regulation of a lipid binding domain in the v-SNARE synaptobrevin and its role in vesicular fusion. Biol. Cell. *95*, 459–464.

Della Rocca, G.J., Mukhin, Y.V., Garnovskaya, M.N., Daaka, Y., Clark, G.J., Luttrell, L.M., Lefkowitz, R.J., and Raymond, J.R. (1999). Serotonin 5-HT1A Receptor-mediated ERK activation requires calcium/calmodulin-dependent receptor endocytosis. J. Biol. Chem. *274*, 4749–4753.

Desrivieres, S., Cooke, F.T., Morales-Johansson, H., Parker, P.J., and Hall, M.N. (2002). Calmodulin controls organization of the actin cytoskeleton via regulation of phosphatidylinositol (4,5)-bisphosphate synthesis in *Saccharomyces cerevisiae*. Biochem. J. *366*, 945–951.

Diaz-Meco, M.T., *et al*. (1993). A dominant negative protein kinase C-zeta subspecies blocks NF-kappa B activation. Mol. Cell. Biol. *13*, 4770–4775.

Diaz-Meco, M.T., Municio, M.M., Pilar, S., Lozano, J., and Moscat, J. (1996). Lambda-interacting protein, a novel protein that specifically interacts with the zinc finger domain of the atypical protein kinase C isotype lambda/iota and stimulates its kinase activity in vitro and in vivo. Mol. Cell. Biol. *16*, 105–114.

Feng, X., Becker, K.P., Stribling, S.D., Peters, K.G., and Hannun, Y.A. (2000). Regulation of receptor-mediated protein kinase C membrane trafficking by autophosphorylation. J. Biol. Chem. *275*, 17024–17034.

Geuze, H.J., Slot, J.W., Strous, G.J., Peppard, J., von Figura, K., Hasilik, A., and Schwartz, A.L. (1984). Intracellular receptor sorting during endocytosis: comparative immunoelectron microscopy of multiple receptors in rat liver. Cell *37*, 195–204.

Grewal, T., Heeren, J., Mewawala, D., Schnitgerhans, T., Wendt, D., Salomon, G., Enrich, C., Beisiegel, U., and Jäckle, S. (2000). Annexin VI stimulates endocytosis and is involved in the trafficking of low density lipoprotein to the prelysosomal compartment. J. Biol. Chem. *275*, 33806–33813.

Gruenberg, J. (2001). The endocytic pathway: a mosaic of domains. Nat. Rev. Mol. Cell. Biol. *2*, 721–730.

Gschwendt, M., Muller, H.J., Kielbassa, K., Zang, R., Kittstein, W., Rincke, G., and Marks, F. (1994). Rottlerin, a novel protein kinase inhibitor. Biochem. Biophys. Res. Commun. *199*, 93–98.

Hall, A. (1994). Small GTP-binding proteins and the regulation of the actin cytoskeleton. Annu. Rev. Cell Biol. *10*, 31–54.

Hirai, I., and Wang, H.G. (2002). A role of C-terminal region of human Rad9 (hRad9) in nuclear transport of the hRad9 check point complex. J. Biol. Chem. *277*, 25722–25727.

Huber, L.A., Fialka, I., Paiha, K., Hunziker, W., Sacks, D.B., Bähler, M., Way, M., Gagescu, R., and Gruenberg, J. (2000). Both calmodulin and the unconventional myosin myr4 regulate membrane trafficking along the recycling pathway of MDCK cells. Traffic *1*, 494–503.

Hunziker, W. (1994) The calmodulin antagonist W-7 affects transcytosis, lysosomal transport, and recycling but not endocytosis. J. Biol. Chem. *269*, 29003–29009.

Iwabu, A., Smith, K., Allen, F.D., Lauffenburger, D.A., and Wells, A. (2004). Epidermal growth factor induces fibroblast contractility and motility via protein kinase C δ-dependent pathway. J. Biol. Chem. *279*, 14551–14560.

Jaken, S., and Parker, P.J. (2000). Protein kinase C binding partners. BioEssays *22*, 245–254.

Keenan, C., and Kelleher, D. (1998). Protein kinase C and the cytoskeleton. Cell Signal. *10*, 225–232.

Kikkawa, U., Matsuzaki, H., and Yamamoto, T. (2002). Protein kinase Cδ (PKCδ): activation mechanisms and functions. J. Biochem. *132*, 831–839.

Klausner, R.D., Harford, J., and Renswoude, J. (1984). Rapid internalization of the tyransferrin receptor in K562 cells is triggered by ligand binding or treatment with phorbol ester. Proc. Natl. Acad. Sci. USA *81*, 3005–3009.

Kornilova, E., Sorkina, T., Beguinot, L., and Sorkin, A. (1996). Lysosomal targeting of EGF receptors via a kinase-dependent pathway is mediated by the receptor carboxyl-terminal residues 1022–1123. J. Biol. Chem. *271*, 30340–30346.

Laemmli, U.K. (1970). Cleavage of structural proteins during the assembly of the head of bacteriophage T4. Nature *227*, 680–685.

Larocca, M.C., Ochoa, E.J., Rodriguez Garay, E.A., and Marinelli, R.A. (2002). Protein kinase C-dependent inhibition of the lysosomal degradation of endocytosed proteins in rat hepatocytes. Cell Signal. *14*, 641–647.

Lawe, D.C., Sitouah, N., Hayes, S., Chawla, A., Virbasius, J.V., Tuft, R., Fogarty, K., Lifshitz, L., Lambright, D., and Corvera, S. (2003). Essential role of Ca^{2+}/calmodulin in early endosome antigen-1 localization. Mol. Biol. Cell *14*, 2935–2945.

Le, T.L., Joseph, S.R., Yap, A.S., and Stow, J.L. (2002). Protein kinase C regulates endocytosis and recycling of E-cadherin. Am. J. Physiol. *283*, C489–C499.

Li, H., Ruano, M.J., and Villalobo, A. (2004). Endogenous calmodulin interacts with the epidermal growth factor receptor in living cells. FEBS Lett. *559*, 175–180.

Li, W., Zhang, J., Bottaro, D.P., Li, W., and Pierce, J.H. (1997). Identification of serine 643 of protein kinase C-δ as an important autophosphorylation site for its enzymatic activity. J. Biol. Chem. *272*, 24550–24555.

Lindberg, L.G., and Vorwerk, P. (1970). On calculating volumes of transected bodies from two-dimensional micrographs. Lab. Investig. *23*, 315–317.

Ling, M., Trollér, U., Zeidman, R., Lundberg, C., and Larsson, C. (2004). Induction of neurites by the regulatory domains of PKCδ and ϵ is counteracted by PKC catalytic activity and by the RhoA pathway. Exp. Cell Res. *292*, 135–150.

Lippincott-Schwartz, J., Yuan, L., Tipper, C., Amherdt, M., Orci, L., and Klausner, R.D. (1991). Brefeldin A's effects on endosomes, lysosomes, and the TGN suggest a general mechanism for regulating organelle structure and membrane traffic. Cell *67*, 601–616.

Liu, Y., Graham, C., Parravicini, V., Brown, M.J., Rivera, J., and Shaw, S. (2001). Protein kinase C theta is expressed in mast cells and is functionally involved in Fcϵ receptor I signaling. J. Leukoc. Biol. *69*, 831–840.

Llorente, A., Garred, O., Holm, P.K., Eker, P., Jacobsen, J., van Deurs, B., and Sandvig, K. (1996). Effect of calmodulin antagonists on endocytosis and intracellular transport of ricin in polarized MDCK cells. Exp. Cell Res. *227*, 298–308.

Lund, K.A., Lazar, C.S., Chen, W.S., Walsch, B.J., Welsh, J.B., Herbst, J.J., Walton, G.M., Rosenfeld, M.G., Gill, G.N., and Wiley, H.S. (1990). Phosphorylation of the epidermal growth factor receptor at threonine 654 inhibits ligand-induced internalization and down-regulation. J. Biol. Chem. *265*, 20517–20523.

Martin-Nieto, J., and Villalobo, A. (1998). The human epidermal growth factor receptor contains a juxtamembrane calmodulin-binding site. Biochemistry *37*, 227–236.

Mayorga, L.S., Berón, W., Sarrouf, M.N., Colombo, M.I., Creutz, C., and Stahl, P.D. (1994). Calcium-dependent fusion among endosomes. J. Biol. Chem. *269*, 30927–30934.

Mori, M.X., Erickson, M.G., and Yue, D.T. (2004). Functional stoichiometry and local enrichment of calmodulin interacting with Ca^{2+} channels. Science *304*, 432–435.

Mochly-Rosen, D., and Gordon, A.S. (1998). Anchoring proteins for protein kinase C: a means for isoenzyme selectivity. FASEB J. *12*, 35–42.

Mu, F.-T., Callaghan, J.M., Steele-Mortimer, O., Stenmark, H., Parton, R.G., Campbell, P.L., McCluskey, J., Yeo, J.-P., Tock, E.P.C., and Toh, B.-H. (1995). EEA1, an early endosome-associated protein. EEA1 is a conserved α-helical peripheral membrane protein flanked by cysteine "fingers" and contains a calmodulin-binding IQ motif. J. Biol. Chem. *270*, 13503–13511.

Newton, A.C. (1997). Regulation of protein kinase C. Curr. Opin. Cell Biol. *9*, 161–167.

Peters, C., and Mayer, A. (1998). Ca^{2+}/calmodulin signals the completion of docking and triggers a late step of vacuole fusion. Nature *396*, 575–580.

Ohmori, S., Shirai, Y., Sakai, N., Fujii, M., Konishi, H., Kikkawa, U., and Saito, N. (1998). Three distinct mechanisms for translocation and activation of the δ subspecies of protein kinase C. Mol. Cell. Biol. *18*, 5263–5271.

Pons, M., Ihrke, G., Koch, S., Biermer, M., Pol, A., Grewal, T., Jäckle, S., and Enrich, C. (2000). Late endocytic compartments are the major sites of annexin VI localisation in NRK fibroblasts and polarised WIF-B hepatoma cells. Exp. Cell Res. *257*, 33–47.

Prevostel, C., Alice, V., Joubert, D., and Parker, P.J. (2000). Protein kinace Cα actively downregulates through caveolae-dependent traffic to an endosomal compartment. J. Cell Sci. *113*, 2575–2584.

Quetglas, S., Leveque, C., Miquelis, R., Sato, K., and Seagar, M. (2000). Ca2+-dependent regulation of synaptic SNARE complex assembly via a calmodulin- and phospholipid-binding domain of synaptobrevin. Proc. Natl. Acad. Sci. USA *97*, 9695–9700.

Ridge, K.M., Dada, L., Lecuona, E., Bertorello, A.M., Katz, A.I., Mochly-Rosen, D., and Sznajder, J.I. (2002). Dopamine-induced exocytosis of Na,K-ATPase is dependent on activation of protein kinase C-ϵ and -δ. Mol. Biol. Cell *13*, 1381–1389.

Ridley, A.J. (2001). Rho proteins, linking signaling with membrane trafficking. Traffic *2*, 303–310.

Saito, N., Kikkawa, U., and Nishizuka, Y. (2002). The family of protein kinase C and membrane lipid mediators. J. Diabetes Complications *16*, 4–8.

San José, E., Benguría, A., Geller, P., and Villalobo, A. (1992). Calmodulin inhibits the epidermal growth factor receptor tyrosine kinase. J. Biol. Chem. *267*, 15237–15245.

Sanchez, P., de Carcer, G., Sandoval, I.V., Moscat, J., and Diaz-Meco, M.T. (1998). Localization of atypical protein kinase C isoforms into lysosome-targeted endosomes through interaction with p62. Mol. Cell. Biol. *18*, 3069–3080.

Schmidt, A., and Hall, M.N. (1998). Signaling to the actin cytoskeleton. Annu. Rev. Cell Biol. *14*, 305–338.

Stempka, L., Schnölzer, M., Radke, S., Rinske, G., Marks, F., and Gschwendt, M. (1999). Requirements of protein kinase Cδ for catalytic function. J. Biol. Chem. *274*, 8886–8892.

Tebar, F., Villalonga, P., Sorkina, T., Agell, N., Sorkin, A., and Enrich, C. (2002). Calmodulin regulates intracellular trafficking of epidermal growth

factor receptor and the MAPK signaling pathway. Mol. Biol. Cell *13*, 2057–2068.

Uberall, F., Giselbrecht, S., Hellbert, K., Fresser, F., Bauer, B., Gschwendt, M., Grunicke, H.H., and Baier, G. (1997). Conventional PKC-alpha, novel PKC-epsilon and PKC-theta, but not atypical PKC-lambda are MARCKS kinases in intact NIH 3T3 fibroblasts. J. Biol. Chem. *272*, 4072–4078.

Ward, N.E., Gravit, K.R., and O'Brian, C.A. (1995). Irreversible inactivation of protein kinase C by a peptide-substrate analog. J. Biol. Chem. *270*, 8056–8060.

Ward, N.E., Gravit, K.R., and O'Brian, C.A. (1996). Covalent modification of protein kinase C isoenzymes by the inactivating peptide substrate analog N-biotinyl-Arg-Arg-Arg-Cys-Leu-Arg-Arg-Leu. Evidence that the biotinylated peptide is an active-site affinity label. J. Biol. Chem. *271*, 24193–24200.

Weibel, E.R. (1979). Stereological Methods, Vol. 1. Practical Methods for Biological Morphometry, London: Academic Press.

Wood, S.A., and Brown, W.J. (1992). The morphology but not the function of endosomes and lysosomes is altered by brefeldin A. J. Cell Biol. *119*, 273–285.

Yoshida, K., Wang, H-G., Miki, Y., and Kufe, D. (2003). Protein kinase Cδ is responsible for constitutive and DNA damage-induced phosphorylation of Rad9. EMBO J. *22*, 1431–1441.